ACS APPLIED MATERIALS & INTERFACES

Research Article

www.acsami.org

Urchinlike Nanostructure of Single-Crystalline Nanorods of Sb_2S_3 Formed at Mild Reaction Condition

Nilkamal Maiti,[†] Sang Hyuk Im,[†] Yong Hui Lee, and Sang Il Seok*

Solar Energy Materials Research Group, Division of Advanced Materials, Korea Research Institute of Chemical Technology, 141 Gajeong-ro, Yuseong, Daejeon

Supporting Information

ABSTRACT: Urchinlike nanostructure of well-defined Sb_2S_3 crystals of 3−4 μm in length and 30−150 nm in diameter oriented along [001] direction have been produced at a mild reaction temperature of 90 °C from $SbCl_3$ and S-methyl 3-phenyldithiocarbazate [$C_6H_5NHNHC(S)SMe$] in ethylene glycol medium. During the reaction, the amorphous Sb_2S_3 spheres of 1.4 μm in diameter were formed at early reaction stage and then crystalline nanorods were continuously grown at the surface of Sb_2S_3 spheres while transforming their morphology into urchinlike structure. The urchinlike Sb_2S_3 was composed of single-crystalline Sb_2S_3 nanorods, belong to the orthorhombic phase with cell parameters a = 11.307 Å, b = 11.278 Å, c = 3.847 Å and absorbed the light up to 750 nm-wavelength region. The urchinlike Sb_2S_3 architecture was applied to the photoelectrochemical cell.

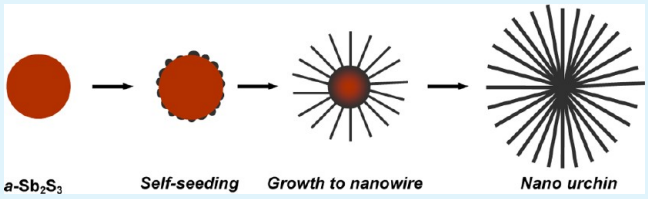

KEYWORDS: *Sb_2S_3, urchinlike structure, S-methyl 3-phenyldithiocarbazate, solvothermal method*

INTRODUCTION

One-dimensional (1D) semiconductor nanocrystalline materials with unique size and morphology has been rapidly explored because of their potential application in fabrication of optical and electronic devices,[1−3] as the properties of nanocrystalline materials are highly dependent on their shape, size, and crystalline phase.

Group V−VI binary crystalline compound, e.g. Sb_2S_3 is highly anisotropic, a kind of layered structure parallel to their growth direction and is a direct band gap semiconductor that crystallizes in the orthorhombic phase.[4−6] The Sb_2S_3 also has unique properties such as high absorption coefficient in visible region, suitable bandgap, and chain-like layered structure[7,8] and consequently it can be used to solar cells,[9−12] photocatalysts,[13,14] thermo-electric cooling devices,[15] Li-storage electrodes,[16] and optoelectronic devices[17] in infrared region.

Therefore, several methods have been developed to synthesize Sb_2S_3 nanomaterials such as solvothermal synthesis for nanorods,[18,19] nanowires,[20] and nanotubes;[21,22] spray pyrolysis[23] and chemical bath deposition[24,25] for thin films; sonochemical method for microcrystal;[26] and so on. Most of all, the useful crystalline Sb_2S_3 (stibnite) should be converted from amorphouse phase of Sb_2S_3 trough relatively high solution temperature in solvothermal synthesis or high furnace temprature in post-heat-treatment after chemical bath deposition because the glass-transition temperature of Sb_2S_3 is ca. 225 °C.[27] Even though it is well-explained that the Sb_2S_3 tends to form 1D structure through solution chemistry, it has overlooked that the final crystalline Sb_2S_3 is formed from the initial amorphous Sb_2S_3 which determins the size and uniforminty of final crystalline Sb_2S_3. In addition, it is still challenging to synthesize the uniform crystalline Sb_2S_3 particles having high surface area for the applications to photocatalyst, Li-storage, and photovoltaic systems and it will be equally important how to conveniently synthesize such crystalline Sb_2S_3 compounds at low temperature, for short time and control the morphology through simple method.

Therefore, here, we would like to introduce a facile approach to synthesized crystalline Sb_2S_3 nanourchin which is composed of single-crystalline Sb_2S_3 nanorods with dimensions of 30−150 nm in diameter and 3.5−4.0 μm in length via solvothermal method using antimony(III) chloride and S-methyl 3-phenyldithiocarbazate [$C_6H_5NHNHC(S)SMe$][28] in ethylene glycol without any surfactants and additives. We have characterized the transformation route of the amorphous Sb_2S_3 spheres to the crystalline urchinlike Sb_2S_3. In addition, the photoelectrochemical cell using the urchinlike Sb_2S_3 as both photoelectrode and light harvester was fabricated.

EXPERIMENTAL SECTION

Preparation of S-Methyl 3-Phenyldithiocarbazate. S-Methyl 3-phenyldithiocarbazate [C6H5NHNHC(S)SMe] was prepared adapting the procedure given in literature.[28] The compound is confirmed by mass spectroscopy, elemental analysis and ^{1}H NMR spectroscopy. Mass: 198 m/z. Anal. Calcd for $C_8H_{10}N_2S_2$: C, 48.45; H, 5.08; N, 14.13; S, 32.34. Found: C, 48.96; H, 5.01; N, 14.18; S, 35.69%. ^{1}H NMR (ppm, acetone d_6) δ: 10.28 (1H, NH); 7.75 (1H, NH); 7.23 (2H); 6.88 (1H); 6.83 (2H) and 2.48 (3H).

Received: June 24, 2012
Accepted: August 6, 2012
Published: August 6, 2012

   dx.doi.org/10.1021/am301141q | ACS Appl. Mater. Interfaces 2012, 4, 4787−4791

Synthesis of Sb_2S_3 Nanourchin. A two necked round-bottom flask (50 mL) was charged with $SbCl_3$ (0.5 g, 2.192 mmol), S-methyl 3-phenyldithiocarbazate (0.434 g. 2.192 mmol), and 20 mL of ethylene glycol. All the reagents were dissolved by stirring. The flask was then degassed for 10 min, filled with argon, and heated at 90 °C for 45 min. During heating, the color of the solution was gradually changed from orange red (t = 20 min), brick red (t = 25 min), and black (t > 30 min). The shape and morphology of the intermediate was examined by picking out the reactant as soon as the color of reactant was distinctively changed. The samples were quenched by dropping in excess ethanol and then were collected by centrifugation, washed with water and ethanol for several times. The final product (t = 45 min) was also collected by centrifugation, washed with water and ethanol several times, and subsequently dried at 60 °C under vacuum.

Fabrication of Sb_2S_3 Urchin-Sensitized Photoelectrochemical Cell. A dense TiO_2 of a 60 nm thickness layer was deposited on FTO (Fluorine doped SnO_2: TEC 8, Pilkington) by spraying 20 mM of titanium diisopropoxide bis(acetylacetonate) solution at 450 °C. We then dropped the above final product solution (t = 45 min) of urchinlike Sb_2S_3 on the TiO_2/FTO film and dried it at 300 °C for 20 min in N_2 atmosphere. The photoelectrochemical cell using urchinlike Sb_2S_3 as both photoelectrode and light harvester was fabricated by sandwiching the Sb_2S_3 urchin/TiO_2/FTO film and Pt-coated counter electrode with a thermal adhesive film (Surlyn, DuPont; thickness, 60 μm). The Pt-coated counter electrode was prepared by dropping 5 mM solution of H_2PtCl_6 in i-propanol on a FTO glass plate and subsequent heating at 400 °C for 10 min. We filled a cobalt electrolyte in the gap of the sandwich cell. The cobalt electrolytes were synthesized by dissolving 0.5 M of Co(II) complex $[Co(o\text{-phen})_3](TFSI)_2$, where o-phen stands for 1,10-phenanthroline and TFSI for bis(trifluoromethanesulfonyl) imide/0.05 M of Co(III) complex $[Co(o\text{-phen})_3](TFSI)_3$, and 0.2 M of lithium perchlorate ($LiClO_4$) in acetonitrile/ethylene carbonate (4/6 v/v).[12] Finally, we made lead contact pads on both sides of the electrode by an ultrasonic soldering iron.

Device Characterization. The external quantum efficiency (EQE) spectrum was measured by a light source (300 W xenon lamp, 66902; Newport) aligned with a monochromator (Cornerstone™ 260; Newport) and a multimeter (Keithley 2001).

RESULTS AND DISCUSSION

The structure and morphology transformation of Sb_2S_3 nanourchin was investigated by checking the TEM image of their intermediates as shown in Figure 1. Figure 1a presented the amorphous Sb_2S_3 particle (average size about 1.4 μm) formed at the early stage of the reaction (t = 20 min) at 90 °C in ethylene glycol. When the reaction proceeds further (t = 25 min), some short buds were created from the surface of the amorphous particles (Figure 1b) and the short buds grown to crystalline small rods by further growth (Figure 1c, t = 30 min). At the final stage of reaction (t = 45 min) under the same reaction conditions, urchinlike shaped Sb_2S_3 composed of nanorods was observed (Figue 1e) (see the SEM images in Figure 1g, h for the amorphous Sb_2S_3 particles and crystalline urchinlike Sb_2S_3 particles). The SEM image of Sb_2S_3 particles (see Figure S1 in the Supporting Information) sampling at t = 35 min, indicates that the amorphous particles with the short crystalline buds are quickly transformed into urchin shape and thus the sphere and urchinlike morphology coexist.

The nanorods were grown with no branching which indicated that the Sb_2S_3 nanorods were believed to be developed from spontaneous nucleation with greater crystal perfections. The rods were grown longer with increasing reaction time. The morphology and composition of the as-grown Sb_2S_3 nanocompound were determined by TEM. Figure 1f is the HRTEM (high-resolution TEM) image of the nanorods obtained from the urchinlike Sb_2S_3 structure. At the

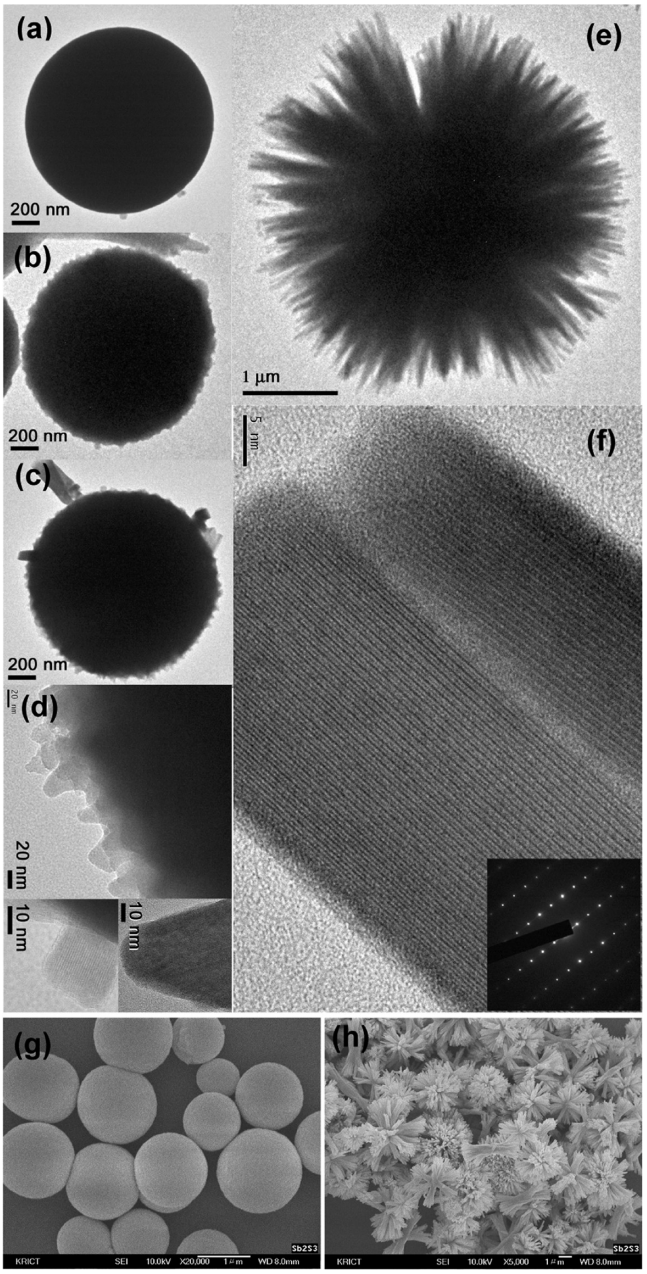

Figure 1. Morphology evolution of the Sb_2S_3 nanourchin. TEM images of (a) spherical amorphous particle at early reaction stage (t = 20 min); (b) seeds on the surface of an amorphous particle (t = 25 min); (c, d) rodlike crystalline growth around the particle and its HRTEM images (t = 30 min); (e, f) nanourchin particles and HRTEM image of each nanowire, inset = SAED pattern of the nanowire (t = 45 min); and SEM images of (g) amorphous Sb_2S_3 particles and (h) crystalline urchinlike Sb_2S_3 particles.

end of the reaction the diameter of the nanorods were in a range from 30−200 nm and lengths in a range from 3.5−4.0 μm. The crystal planes, parallel to the rod axis, have spacings of 0.375 nm, which match well with the distance between the neighboring lattices of the (001) planes. This result verifies that the preferential growth occurred along the [001] direction. An EDX spectrum of Sb_2S_3 nanourchin in Figure 2b shows that the nanourchin is composed to the compound of Sb:S = 1:1.32. Here, it should be noted that the crystalline Sb_2S_3 nanourchin could be synthesized at mild reaction temperature (90 °C) by

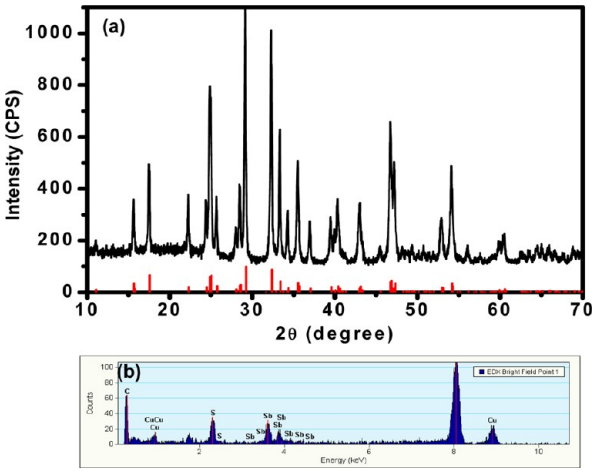

Figure 2. (a) XRD pattern of the as-prepares Sb_2S_3 obtained at 90 °C for 45 min (upper) and standard stick pattern for orthorhombic Sb_2S_3 (lower, JCPDS no. 03−065−2432) and (b) its EDX spectrum.

this simple solution chemistry. The phase and crystallographic orientation of the urchinlike Sb_2S_3 product were identified by XRD analysis as shown in Figure 2a. On the basis of XRD analysis from urchinlike compound, the crystallographic phase of the Sb_2S_3 nanorods can be readily indexed to the orthorhombic phase having calculated cell parameters of a = 11.307 Å, b = 11.278 Å, c = 3.847 Å, which are in agreement with the published JCPDS data no. 03−065−2432. No peak corresponding to metallic Sb, or oxides of antimony were observed. The strong intensity and narrow width of the Sb_2S_3 diffraction peaks indicated that the as-grown nanowires are highly pure and well-developed single crystals. From the Scherrer's equation, we know that the urchinlike Sb_2S_3 is ∼50 nm in the crystalline size and single crystal owing to the similarity in the diameter of Sb_2S_3 nanorods (see the TEM image of Sb_2S_3 nanorods separated from the urchinlike structure in Figure S2 in the Supporting Information).

The various influences on the formation of urchinlike structure were investigated. In our experiment, first $SbCl_3$ and $C_6H_5NHNHC(S)SMe$ were dissolved in ethylene glycol by stirring. In this stage, no color change was observed. In a typical heating process at 90 °C, the solution becomes orange red (after 20 min) in the color due to formation of amorphous antimony sulfide nano particles with about 1.4 μm in size (Figure 1a) and then finally to black coloration, with increasing reaction time. When the same reaction is carried out at about 75 °C, only amorphous Sb_2S_3 was generated. On the other hand, when we have used ethanol in place of ethylene glycol, the color of the solution first changed to yellow, possibly because of formation of $Sb[C_6H_5NHNHC(S)SMe]_3$ and then to orange red due to formation of amorphous Sb_2S_3,[29] but the crystalline Sb_2S_3 was not formed even for long time reaction period. These results indicate that the Sb^{3+} ion first solvated by polyol chelating solvent, ethylene glycol, formed solvated antimony intermediate compound which is relatively stable than that of antimony-dithiocarbazate complex.[30] In the early stage of solvothermal process at low temperature, the well-controlled release of Sb^{3+} ions from solvated antimony intermediate as well as the well controlled generation of S^{2-} from $C_6H_5NHNHC(S)SMe$[30,31] seem to lead the formation of relatively uniform amorphous Sb_2S_3 particles (Figure 1a) which becoming urchinlike structure when subsequent nucleation and preferential growth of crystallization occur simultaneously with time under same reaction condition. Figure 3 illustrates the schematic mechanism of such transformation.

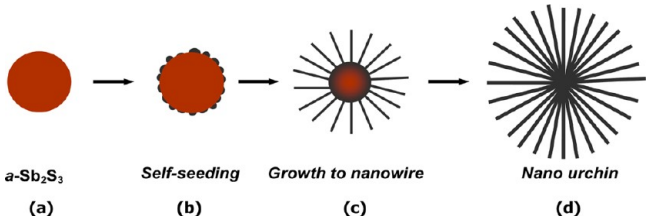

Figure 3. Schematic illustration of the growth mechanism of urchinlike Sb_2S_3 nanostructure: (a) spherical amorphous particle, (b) formation of small seeds (or nuclei) on surface of the particle, (c) small rodlike growth around the particle, and (d) urchinlike structure.

The possible mechanism for the formation of urchinlike Sb_2S_3 nano structure are expected to proceed through two stages, nucleation or seed formation and crystal growth. In the first stage, under solvothermal conditions (sulfur source, solvent, reaction temperature, reaction time, pressure, and so on),[32−34] the amorphous particles underwent disruption and large numbers of small nanocrystallites of Sb_2S_3, which were served as nuclei or seeds, were generated on the surfaces of the amorphous particles (Figure 1b). In the second stage, as a result of solvothermal ripening, these nanocrystalline seeds individually grow preferentially along energetically favorable directions with relatively high concentrations of amorphous Sb_2S_3 and becoming small rod-like (Figure 1c) through a solid−solution−solid (called SSS) transformation mechanism.[35] Accordingly, one small rod-like particle after another was created and then diffuses to bigger one maintaining the growing structure under the Sb−S atom chain anisotropy (i.e., anisotropic chain structure of Sb_2S_3, Figure 4) and non-equilibrium growth condition.[29,36,37]

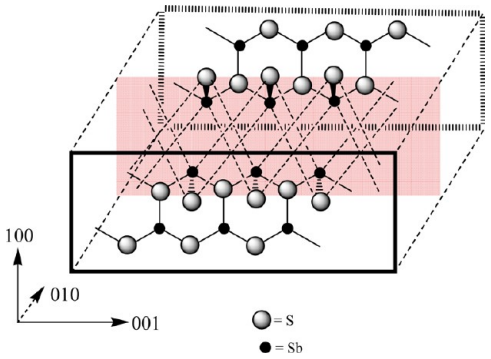

Figure 4. Parallel chain structure of Sb_2S_3 viewed along the [010] direction. The dashed lines (---) indicate weak van der Waals bonds and the cleavage trace is defined by the brown shadow.

The Sb−S chain anisotropy and nonequilibrium growth condition of stibnite Sb_2S_3 can be explained by considering its infinite parallel chain-like $(Sb_4S_6)_n$ framework (Figure 4), in which each parallel chain consists of two types of Sb and three types of S atoms.[30] Both of the Sb atoms are predicted to be Sb^{3+}.[38] Among the two types of Sb atoms, one is formally tri-coordinated and connected to the three S atoms by strongly covalent bonds within a chain and the remaining Sb atom is formally penta-coordinated and connected to the five S atoms,

dx.doi.org/10.1021/am301141q | ACS Appl. Mater. Interfaces 2012, 4, 4787−4791

of which three S atoms are by strongly covalent bonds (within the same chain) and remaining two S atoms are by weaker van der Waals bonds to the next parallel running chain.[39] Only the van der Waals bonds are responsible for the cleavage of the crystal. Thus perfect cleavage of the crystal takes place parallel to the [010] planes where only van der Waals bonds are broken. As a result of Sb−S atom chain asymmetry, the Sb_2S_3 nanorods are growing along the [001] direction, which is also supported by our HRTEM observation in Figure 1f. Thus the nuclei play an important role for the growth of nanowires until the end of either antimony or sulfur source. Thus from each Sb_2S_3 particle, there are several nanowires on the outer surface as a result of urchinlike structure.

Finally, urchinlike nanostructure of single-crystalline nanorods of Sb_2S_3 was applied to the photoelectrochemical cell, consisted of a FTO/thin-TiO_2/Sb_2S_3 urchin/cobalt electrolyte/Pt as transparent electrode/electron conductor/sensitizer/redox electrolyte/counter electrode layer. Figure 5a shows the

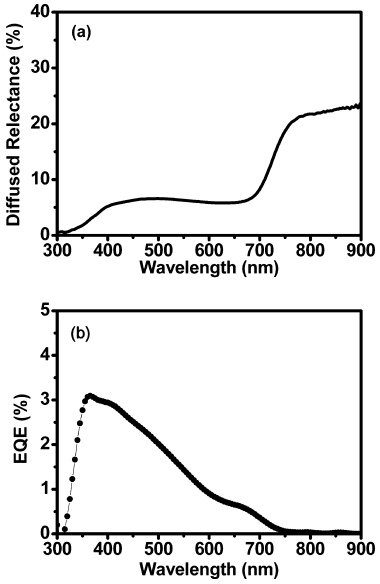

Figure 5. (a) Diffused reflectance of Sb_2S_3 urchin/TiO_2/FTO film and (b) EQE spectrum of Sb_2S_3 urchin-sensitized photoelectrochemical cell.

diffused reflectance of urchinlike Sb_2S_3 deposited on a dense and thin TiO_2 layer. We see that the Sb_2S_3 nanourchin absorbs the light up to 750 nm-wavelength region. The EQE spectrum of Figure 5b confirms that urchinlike Sb_2S_3 architecture can be used as photoelectrode to convert a light energy into electricity by further optimization.

CONCLUSIONS

The Sb_2S_3 nanourchin particles composed of Sb_2S_3 nanorods have been successfully synthesized from $SbCl_3$ and S-methyl 3-phenyldithiocarbazate [$C_6H_5NHNHC(S)SMe$] via a simple solvothermal process in ethylene glycol at 90 °C. The experimental results of the as-grown product showed that the crystal structure, shape and size strongly depend on solvent, reaction temperature and reaction time. At the initial stage of reaction, spherical amorphous Sb_2S_3 particles were generated. With increasing the reaction time, small nanorods were formed and gradually grew outward on the particles, consequently forming the urchinlike Sb_2S_3, composed of radially grown single-crystalline Sb_2S_3 nanorods having dimension of 30−150 nm in diameter and 3.5−4.0 μm in length. Urchinlike nanostructure of single-crystalline nanorods of Sb_2S_3 can be applied to fabricate photoelectrochemical cell. We believe that these crystalline Sb_2S_3 nanourchin particles will be useful to the fields requiring high surface area such as photocatalyst, Li-storage, and photoelectrochemical devices through the rational design of device architecture.

ASSOCIATED CONTENT

Supporting Information

Additional SEM and TEM images (PDF). This material is available free of charge via the Internet at http://pubs.acs.org.

AUTHOR INFORMATION

Corresponding Author

*To E-mail: seoksi@krict.re.kr.

Author Contributions

†These authors have contributed equally to this work.

Notes

The authors declare no competing financial interest.

ACKNOWLEDGMENTS

This study was supported by the Global Research Laboratory (GRL) Program and the Global Frontier R&D Program on Center for Multiscale Energy System funded by the National Research Foundation under the Ministry of Education, Science and Technology of Korea, and by a grant from the KRICT 2020 Program for Future Technology of the Korea Research Institute of Chemical Technology (KRICT), Republic of Korea.

REFERENCES

(1) Dabbousi, B. O.; Bawendi, M. G.; Onitsuka, O.; Rubner, M. F. *Appl. Phys. Lett.* **1995**, *66*, 1316−1318.
(2) Colvin, V. L.; Schlamp., M. C.; Alivisatos, A. P. *Nature* **1994**, *370*, 354−357.
(3) Klein, D. L.; Roth, R.; Lim, A. K. L.; Alivisatos, A. P.; McEuen, P. L. *Nature* **1997**, *389*, 699−701.
(4) Yu, Y.; Jin, C. H.; Wang, R. H.; Chen, Q.; Peng, L. M. *J. Phys. Chem. B* **2005**, *109*, 18772−18776.
(5) Yu, Y.; Jin, C. H.; Wang, R. H.; Chen, Q.; Peng, L. M. *J. Phys. Chem. B* **2005**, *109*, 23312−23315.
(6) Yu, Y.; Jin, C. H.; Wang, R. H.; Chen, Q.; Peng, L. M. *J. Phys. Chem. B* **2006**, *110*, 13415−13419.
(7) Zakaznova-Herzog, V. P.; Harmer, S. L.; Nesbitt, H. W.; Bancroft, G. M.; Flemming, R.; Pratt, A. R. *Surf. Sci.* **2006**, *600*, 348−356.
(8) Wang, X.; liebau, X. F. *Acta Crystallogr., Sect. B* **1996**, *52*, 7−15.
(9) Itzhaik, Y.; Niitsoo, O.; Page, M.; Hodes, G. *J. Phys. Chem. C.* **2009**, *113*, 4254−4256.
(10) Moon, S.-J.; Itzhaik, Y.; Yum, J.-H.; Zakeeruddin, S. M.; Hodes, G.; Grätzel, M. *J. Phys. Chem. Lett.* **2010**, *1*, 1524−1527.
(11) Chang, J. A.; Rhee, J. H.; Im, S. H.; Lee, Y. H.; Kim, H.-j.; Seok, S. I.; Nazeeruddin, Md. K.; Gratzel, M. *Nano Lett.* **2010**, *10*, 2609−2612.
(12) Im, S. H.; Kim, H. -j.; Lim, C. −S.; Seok, S. I. *Energy Environ. Sci.* **2011**, *4*, 2799−2802.
(13) Sun, M.; Li, D.; Li, W.; Chen, Y.; Chen, Z.; He, Y.; Fu, X. *J. Phys. Chem. C* **2008**, *112*, 18076−18081.
(14) Li, K.-Q.; Huang, F.-Q.; Lin, X.-P. *Scr. Mater.* **2008**, *58*, 834−837.
(15) Roy, B.; Chakraborty, B. R.; Bhattacharya, R.; Dutta, A. K. *Solid State Commun.* **1978**, *25*, 937−940.
(16) Ma, J.; Duan, X.; Lian, J.; Kim, T.; Peng, P.; Liu, X.; Liu, Z.; Li, H.; Zheng, W. *Chem.—Eur. J.* **2010**, *16*, 13210−13217.
(17) Grozdanov, I. *Semicond. Sci. Technol.* **1994**, *9*, 1234−1241.

(18) Mo, M. S.; Zhu, Z. Y.; Yang, X. G.; Liu, X. Y.; Zhang, S. Y.; Gao, J.; Qian, Y. T. *J. Cryst. Growth* **2003**, *256*, 377−382.
(19) Li, C.; Yang, X. G.; Liu, Y. F.; Zhao, Z. Y.; Qian, Y. T. *J. Cryst. Growth* **2003**, *255*, 342−347.
(20) Shen, G. Z.; Chen, D.; Tang, K. B.; Jiang, X.; Qian, Y. T. *J. Cryst. Growth* **2003**, *252*, 350−354.
(21) Zheng, X. W.; Xie, Y.; Zhu, L. Y.; Jiang, X. C.; Jia, Y. B.; Song, W. H.; Sun, Y. P. *Inorg. Chem.* **2002**, *41*, 455−461.
(22) Yang, Q.; Tang, K. B.; Wang, C. R.; Qian, Y. T.; Yu, W. C.; Zhou, G. E.; Li, F. Q. *J. Mater. Chem.* **2001**, *11*, 257−259.
(23) Bhosale, C. H.; Uplane, M. D.; Patil, P. S.; Lockhande, C. D. *Thin Solid Films* **1994**, *248*, 137−139.
(24) Nair, M. T. S.; Peña, Y.; Campos, J.; García, V. M.; Nair, P. K. *J. Electrochem. Soc.* **1998**, *145*, 2113−2120.
(25) Messina, S.; Nair, M. T. S.; Nair, P. K. *Thin Solid Films* **2009**, *517*, 2503−2507.
(26) Zhang, J. H.; Chen, Z.; Wang, Z. L.; Ming, N. B. *J. Mater. Res.* **2008**, *8*, 1804−1808.
(27) Versavel, M. Y.; Haber, J. A. *Thin Solid Films* **2007**, *515*, 7171−7176.
(28) Attanasio, D.; Fares, V.; Imperatori, P.; Mattogno, G.; Tarli, F. *J. Chem. Soc., Dalton Trans.* **1988**, 1217−1223.
(29) Yang, J.; Zeng, J. H.; Yu, S. H.; Yang, L.; Zhang, Y. H.; Qian, Y. T. *Chem. Mater.* **2000**, *12*, 2924−2929.
(30) Bera, P.; Seok, S. I. *J. Nanopart. Res.* **2011**, *13*, 1889−1896.
(31) Bera, P.; Kim, C. H.; Seok, S. I. *polyhedron* **2008**, *27*, 3433−3438.
(32) Hu, H.; Liu, Z.; Yang, B.; Mo, M.; Li, Q.; Yu, W.; Qian, Y. *J. Cryst. Growth* **2004**, *262*, 375−382.
(33) Sheldrick, W. S.; Wachhold, M. *Angew. Chem., Int. Ed.* **1997**, *36*, 206−224.
(34) Zhang, R.; Chen, X.; Mo, M.; Wang, Z.; Zhang, M.; Liu, X.; Qian, Y. *J. Cryst. Growth* **2004**, *262*, 449−455.
(35) Gates, B.; Yin, Y.; Xia, Y. *J. Am. Chem. Soc.* **2000**, *122*, 12582−12583.
(36) Chen, G. Y.; Dneg, B.; Cai, G. B.; Zhang, T. K.; Dong, W. F.; Zhang, W. X.; Xu, A. W. *J. Phys. Chem. C* **2008**, *112*, 672−679.
(37) Wells, A. F. *Inorganic Chemistry*; New York, 1977; Chapter 20, p 907.
(38) Wang, X.; Liebau, X. F. *Acta Crystallogr., Sect. B* **1996**, *52*, 7−15.
(39) Herzog, V. P. Z.; Harmer, S. L.; Nesbitt, H. W.; Bancroft, G. M.; Flemming, R.; Pratt, A. R. *Sulf. Sci.* **2006**, *600*, 348−356.